Theoretical and Experimental Study of Measurement of Microwave Permittivity Using Open Ended Elliptical Coaxial Probes

Yansheng Xu, Fadhel M. Ghannouchi, *Member, IEEE*, and Renato G. Bosisio, *Senior Member, IEEE*

Abstract—**In this paper, a new kind of coaxial probe for measurement of microwave permittivity—open-ended elliptical aperture—is studied from theoretical and experimental view points. Calculated results are discussed and compared with experimental values. Wideband measurements of the dielectric constants of liquids are performed by using this kind of needle type probe. Both theory and experiment show that open-ended elliptical coaxial probes can be successfully used in wideband dielectric constant measurements with the advantage of increased sensitivity, especially at low frequencies. Moreover, this kind of probe can easily be fitted into gels and living tissues: these features are very important in biological applications both for measurements and microwave radiation treatment [1].**

Introduction

MEASUREMENT of microwave permittivity by using standard open-ended coaxial lines has been studied by many authors [2]–[4] and has found useful applications. Because of their simplicity, only coaxial lines with circular configuration have been used. Nevertheless, it is both of theoretical and practical importance to examine probes of more complicated configurations to find new possibilities and advantages. To this end, we shall study open-ended elliptical coaxial probes to improve the sensitivity of measurements, and to facilitate *in vivo* measurements of biological tissues, etc.

Theoretical Analysis

At first, we examine the radiation from an open-ended elliptical coaxial line with an infinite flange. The cross-section of this coaxial line is shown in Fig. 1. The semi-major and semi-minor axes of the ellipses which characterize the dimensions of the inner and outer conductors of the coaxial line are a_1, a_o, b_1 and b_o, respectively.

Manuscript received March 21, 1991; revised June 18, 1991.

Y. Xu is with the Beijing Institute of Radio Measurements, P.O. Box 3923, Beijing, China.

F. M. Ghannouchi and R. G. Bosisio are with Department de genie electrique, Ecole Polytechnique de Montreal, C.P., 6079, succursale A, Montreal, PQ, Canada.

IEEE Log Number 9102820.

The radiated magnetic field of the outside space region is related to the tangential electric field of the aperture $E_{\xi 1}(\xi_1, \eta_1)$ as follows [5]:

$$\vec{H}(\xi,\eta,z) = \frac{i}{2\pi\omega\mu}\int_{S_1}(\nabla\nabla\cdot + k^2)E_{\xi_1}(\xi_1,\eta_1)\frac{e^{ikr}}{r}\left(\vec{i}_{\xi 1}\times i_z\right)ds_1. \tag{1}$$

where

$$r = \left[(x-x_1)^2+(y-y_1)^2\right]^{1/2}, \quad k = \frac{2\pi}{\lambda_o}\sqrt{\epsilon\mu},$$

λ_o is wavelength in free space, ϵ, μ are dielectric constant and permeability of the outside space, respectively and $\vec{i}_{\xi_1}, \vec{i}_z$ are the unit vectors along the ξ_1 and z axes, respectively.

In (1) the electric field $E_{\xi_1}(\xi_1, \eta_1)$ is taken to be the principal mode of the coaxial line and it has only the ξ_1 component [6].

The integration in (1) is performed over the aperture of the coaxial line S_1. The η components of the magnetic fields of the coaxial line are expressed as follows:

$$H_\eta(\xi,\eta,z) = A_o H_{\eta o}\left(e^{ik_i z} - R_o e^{-ik_i z}\right) + \sum_{n=1}^{\infty} A_n R_n(\xi,\eta)\exp(\gamma_n z), \tag{2}$$

where $H_{\eta o}$ denotes the magnetic field of the principal mode with A_o as its coefficient, $A_n R_n(\xi, \eta)$ describe the fields of higher order modes and

$$k_i = k_o\sqrt{\epsilon_t} = \frac{2\pi}{\lambda_o}\sqrt{\epsilon_t},$$

where ϵ_t is the dielectric constant of the medium situated between the inner and outer conductors of the coaxial line.

For E-waves the ξ-component of the electric field is computed to be

$$i\omega\epsilon E_\xi(\xi,\eta,z) = \frac{\delta}{\delta z}H_\eta(\xi,\eta,z). \tag{3}$$

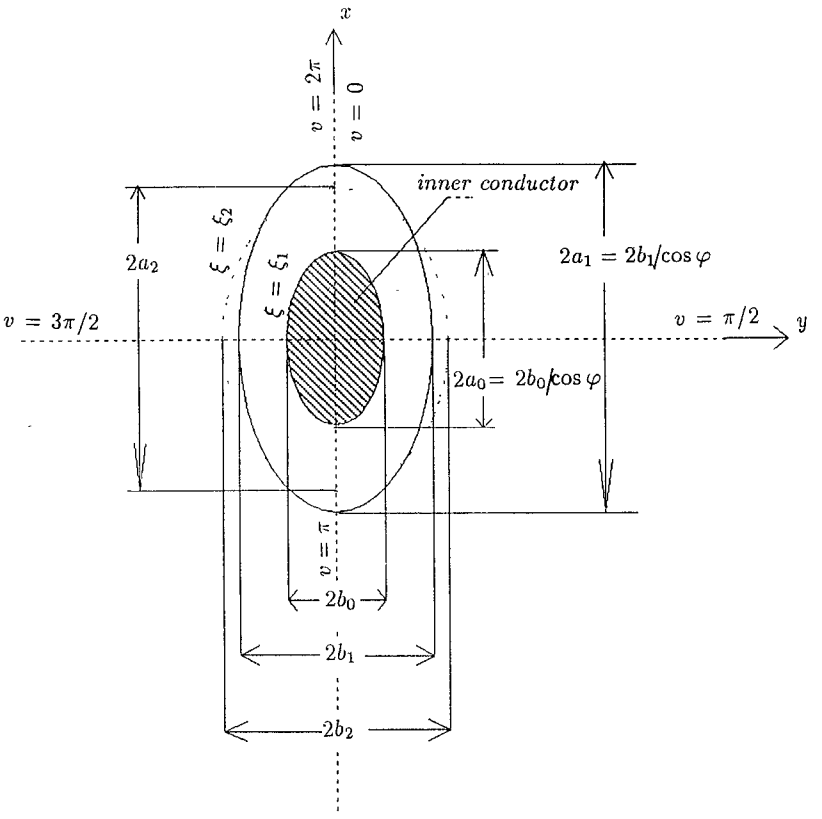

Fig. 1. Cross-section of the elliptic coaxial line, $\xi = \cosh u$, $\eta = \cos v$.

Only the E-modes among the higher order modes are considered at this step discontinuity.

The amplitudes A_n are related to the aperture field $E_{\xi_o}(\xi,\eta)$, and they are obtained by multiplying $E_{\xi}(\xi,\eta)$ with $H_{\eta o}\,ds$ and $R_n(\xi,\eta)\,ds$, respectively. Integration over the aperture gives

$$A_n = \frac{i\omega\epsilon_t \int_S E_{\xi o}(\xi,\eta)\,R_n(\xi,\eta)\,ds}{\gamma_n}$$

and

$$A_o = \frac{\omega\epsilon_t}{k_i}\,\frac{\int_S E_{\xi o}(\xi,\eta)\,H_{\eta o}(\xi,\eta)\,ds}{(1+R_o)\int_S \left[H_{\eta o}(\xi,\eta)\right]^2 ds}. \tag{4}$$

The tangential magnetic fields are continuous in the aperture at $z=0$, and $H_\eta(\xi,\eta,o)$ of (1) is also equal to expression given in (2) over the aperture. We obtain the normalized admittance of the coaxial line by multiplying them by $\vec{i}_\eta H_{\eta o}(\xi,\eta)$ and integrating over the aperture,

$$Y_s = \frac{1-R_0}{1+R_0} = \frac{i\int_S H_{\eta o}(\xi,\eta)\int_{S_1} E_{\xi_1}(\xi_1,\eta_1)\vec{i}_\eta\cdot(\nabla\nabla\cdot + k^2)\dfrac{e^{ikr}}{r}\left(\vec{i}_{\xi_1}\times\vec{i}_z\right)ds_1\,ds}{2\pi\sqrt{\epsilon_t}\,k_o\int_S E_\xi(\xi,\eta)\,H_{\eta o}(\xi,\eta)\,ds}. \tag{5}$$

where $\vec{i}_\eta$ is the unit vector along the η-axis.

In practical measurements very small probes are used and the cross-sections of the probes are generally much smaller than the wavelength. Therefore, all the higher order modes in our calculation may be neglected and in the derivation of (5), the electric field $E_{\xi o}$ is taken to be the principal mode of the coaxial line and hence all terms containing A_n are equal to zero.

It should be pointed out also that the effect of the higher modes may be calculated by using the method, similar to that used in [13], although the computation will be very complicated. The magnetic fields of the principal mode have only one η-component and from references [6], [7] we have

$$H_{\eta o}(\xi,\eta) \sim \frac{A}{\sqrt{\cosh^2 u - \cos^2 v}} = \frac{A}{\sqrt{\xi^2-\eta^2}}, \tag{6}$$

where $\cosh u = \xi$ and $\cos v = \eta$ and A is the amplitude of the magnetic field to be determined.

It is shown that for an arbitrary function $f(\xi,\eta)$, the following integral over the aperture of the coaxial line S

vanishes, i.e.:

$$\begin{aligned}
&\int_S H_{\eta o}(\xi,\eta)\vec{i}_\eta\cdot\nabla f(\xi,\eta)\,ds \\
&= \int_{\xi_1}^{\xi_2}\int_{\upsilon=0}^{\upsilon=2\pi} H_{\eta o}(\xi,\eta)\frac{1}{h\eta}\left[\frac{\delta}{\delta\eta}f(\xi,\eta)\right]h_\xi h_\eta\,d\xi\,d(\cos\upsilon) \\
&= \int_{\xi_1}^{\xi_2}\int_{\upsilon=0}^{\upsilon=2\pi}\frac{\mathrm{AC}}{\sqrt{\xi^2-1}}\frac{\delta}{\delta\eta}f(\xi,\eta)\,d\xi\,d(\cos\upsilon) \\
&= \int_{\xi_1}^{\xi_2}\frac{\mathrm{AC}}{\sqrt{\xi^2-1}}f(\xi,\eta)\Big|_{\upsilon=0}^{\upsilon=2\pi}d\xi \\
&= 0, \qquad (7)
\end{aligned}$$

where h_ξ, h_η are the metrical coefficients of the elliptic coordinates [3]

$$h_\xi = C\sqrt{\frac{\xi^2-\eta^2}{\xi^2-1}}, \qquad h_\eta = C\sqrt{\frac{\xi^2-\eta^2}{1-\eta^2}},$$

and ξ_1, ξ_2 are the coordinates of the inner and outer ellipses, respectively.

The first term on the right hand side of (5) becomes zero and we have

$$Y_s = \frac{ik_o\epsilon\int_S\frac{1}{\sqrt{\xi^2-\eta^2}}\int_{S_1}\frac{1}{\sqrt{\xi_1^2-\eta_1^2}}\frac{e^{\iota kr}}{r}\vec{i}_\eta\cdot\left(\vec{i}_{\xi_1}\times\vec{i}_z\right)ds_1\,ds}{2\pi\sqrt{\epsilon_t}\int_S\frac{1}{(\xi^2-\eta^2)}ds}, \qquad (8)$$

where the field components E_ξ and H_η of the principal mode from [6] are proportional to

$$\frac{1}{\sqrt{\xi^2-\eta^2}}.$$

In order to facilitate the calculation of the value Y_s, we take the cylindrical coordinates (ρ,θ,z) instead of elliptic ones and we have from [7]:

$$X = C\xi\eta, \qquad y = C\sqrt{(\xi^2-1)(1-\eta^2)},$$

$$X = \rho\cos\theta, \qquad y = \rho\sin\theta,$$

$$\rho^2 = X^2 + y^2 + C^2(\xi^2+\eta^2-1),$$

and

$$\frac{X^2}{\eta^2} - \frac{y^2}{1-\eta^2} = C^2.$$

From the above expressions, the following identities can be derived:

$$\xi^2 = \frac{(C^2+\rho^2)+\sqrt{(C^2+\rho^2)^2-4C^2\rho^2\cos^2\theta}}{2C^2}$$

$$\eta^2 = \frac{(C^2+\rho^2)-\sqrt{(C^2+\rho^2)^2-4C^2\rho^2\cos^2\theta}}{C^2}$$

$$\xi_1^2-\eta_1^2 = \frac{\sqrt{(C^2+\rho_1^2)^2-4C^2\rho_1^2\cos^2\theta_1}}{C^2}$$

and $\quad r = \left[\rho^2+\rho_1^2-2\rho\rho_1\cos(\theta-\theta_1)\right]^{1/2}.$

Finally we obtain

$$Y_s = \frac{ik_o\epsilon}{2\pi\sqrt{\epsilon_t}}I = G_s + iB_s$$

where

$$I = \frac{\int_S\frac{1}{\sqrt{\xi^2-\eta^2}}\int_{S_1}\frac{1}{\sqrt{\xi_1^2-\eta_1^2}}\frac{e^{ikr}}{r}\cos\psi\,ds_1\,ds}{\int_S\frac{1}{(\xi^2-\eta^2)}ds}, \qquad (9)$$

and $\psi = \alpha - \alpha_1$ where α and α_1 are the angles between the x-axis and the tangential of the curves ξ = constant and ξ_1 = constant, respectively, the expressions for α and α_1 are given by

$$\alpha = \tan^{-1}\frac{\xi}{\eta}\sqrt{\frac{1-\eta^2}{\xi^2-1}} \quad \text{and} \quad \alpha_1 = \tan^{-1}\frac{\xi_1}{\eta_1}\sqrt{\frac{1-\eta_1^2}{\xi_1^2-1}}.$$

For small probes $|kr| \ll 1$ we may expand e^{ikr} into a Taylor series [8]. The first and third terms of the expansion take the following form (the second term of expansion equals zero):

$$I_1 = \frac{\int_S\frac{1}{\sqrt{\xi^2-\eta^2}}\int_{S_1}\frac{1}{\sqrt{\xi_1^2-\eta_1^2}}\frac{\cos\psi}{r}ds_1\,ds}{\int_S\frac{1}{(\xi^2-\eta^2)}ds}, \qquad (10)$$

$$I_3 = \frac{\int_S\frac{1}{\sqrt{\xi^2-\eta^2}}\int_{S_1}\frac{1}{\sqrt{\xi_1^2-\eta_1^2}}r\cos\psi\,ds_1\,ds}{\int_S\frac{1}{(\xi^2-\eta^2)}ds}, \qquad (11)$$

and $\quad I = I_1 - k^2I_3/2.$

In practice, the fabrication of an elliptic coaxial line is quite complicated, and a simple method to obtain the

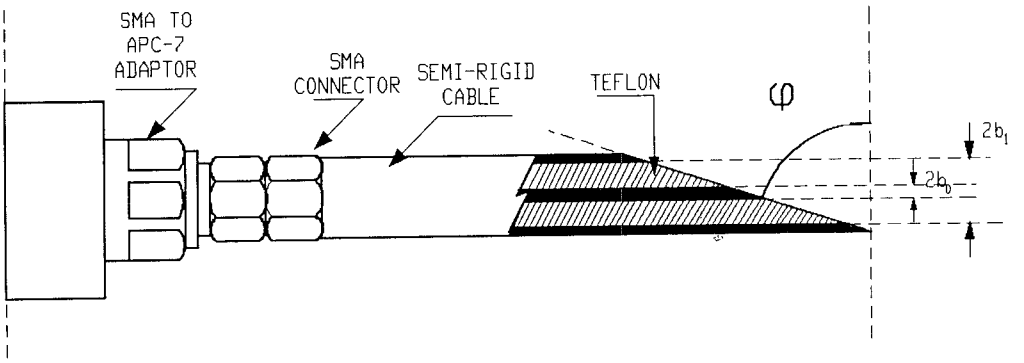

Fig. 2. Coaxial probe with bevel angle.

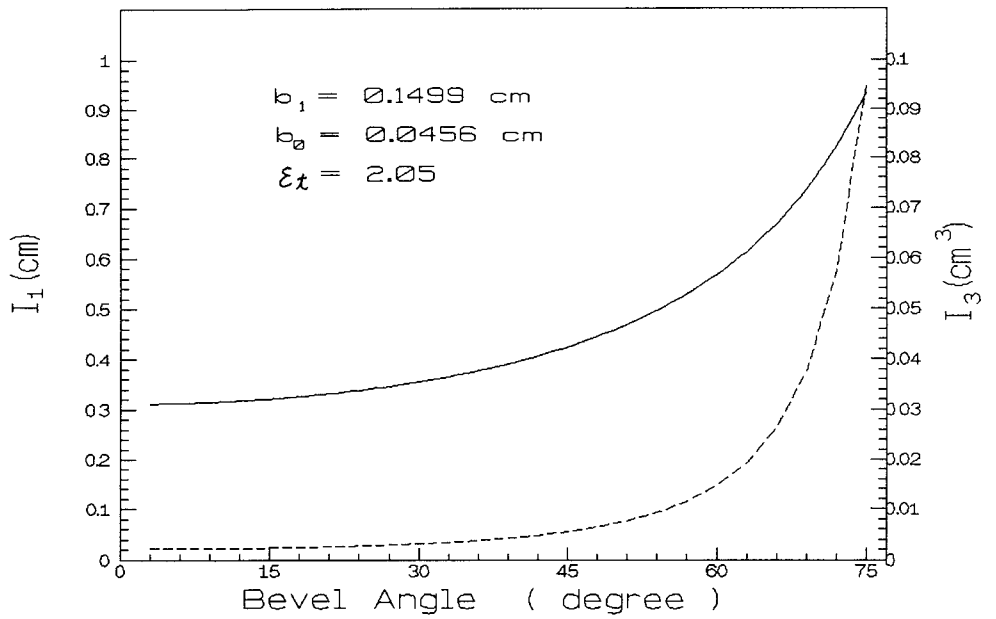

Fig. 3. Calculated curve of integral I_1 and I_3 for different bevel angles. (___ for I_1 and ------ for I_3).

TABLE I
CALCULATED VALUES OF Y_s FOR BEVEL ANGLES 0°, 30°, 45°, AND 60°, $\epsilon = 76 - i11.5$ (WATER), $b_o = 0.0456$ cm AND $b_1 = 0.1499$ cm*

Frequency GHz	$\varphi = 0°$		$\varphi = 30°$		$\varphi = 45°$		$\varphi = 60°$	
	B_s	G_s	B_s	G_s	B_s	G_s	B_s	G_s
2.0	.3240	6.176×10^{-3}	.3736	9.838×10^{-3}	.4532	1.938×10^{-2}	.6276	6.211×10^{-2}
2.5	.3299	1.096×10^{-2}	.3806	1.743×10^{-2}	.4649	3.407×10^{-2}	.6422	.1047
3.0	.3362	1.747×10^{-2}	.3888	2.767×10^{-2}	.4758	5.340×10^{-2}	.6474	.1555
3.5	.3426	2.580×10^{-2}	.3967	4.060×10^{-2}	.4845	7.704×10^{-2}	.6408	.2103
4.0	.3487	3.595×10^{-2}	.4036	5.611×10^{-2}	.4898	.1043	.6218	.2648

*The dielectric constant of water is rather high and the radiation effect is seen from G_s values to become significant at high frequencies and for large bevel angles.

elliptic configuration is to bevel the open-end of a circular coaxial line [9], [10], as shown in Fig. 2. The resulting aperture may be considered as a transition from circular to elliptic and the radiation aperture becomes elliptic also. Although the cross-section of the open-ended circular coaxial probe with bevel angle φ is elliptic, the inner and outer ellipses of the aperture of the probe do not coincide simultaneously with the commonly used elliptic coordinates [7]. To simplify the calculation, an assumption is made to lightly deform the outer ellipse so as to make it coincide with the elliptic coordinates [7] of the inner ellipse. The equal area principle—to make the areas of the ellipses before and after deformation equal to each other—is used, i.e.:

$$a_2 b_2 = a_1 b_1 = a_1^2 \cos\varphi, \tag{12}$$

where a_1, b_1 and a_2, b_2 are the major and minor semi-axis of the outer ellipse before and after deformation, respectively. For elliptic coordinates we have from [7]:

$$C^2 = a_2^2 - b_2^2 = a_o^2 - b_o^2 = a_o^2 \sin^2\varphi,$$

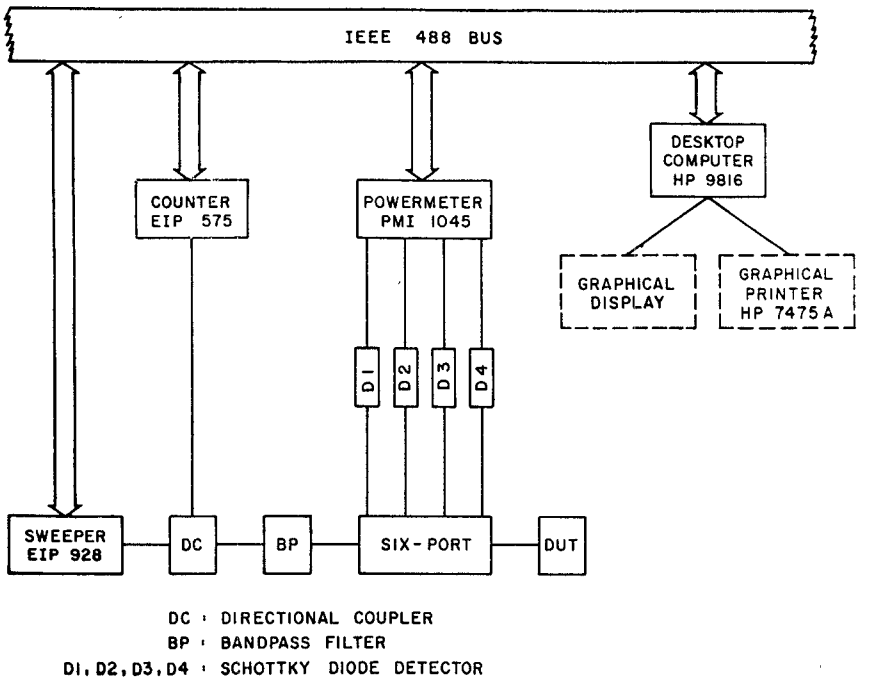

Fig. 4. Block diagram of permittivity measurement system.

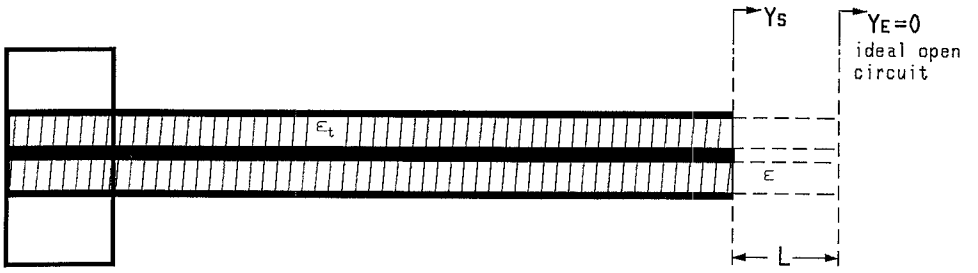

Fig. 5. Model of the probe for measurement.

therefore,

$$C = a_o \sin \varphi. \tag{13}$$

Equations (12) and (13) are solved for a_2, and we find

$$a_2 = \sqrt{\frac{C^2 + \sqrt{C^4 + 4a_1^4 \cos^2 \varphi}}{2}}. \tag{14}$$

The calculated curves of I_1 and I_3 for a circular coaxial line with inner radius $b_o = 0.0456$ cm, outer radius $b_1 = 0.1499$ cm, $\epsilon_t = 2.05$, and different bevel angles φ are shown in Fig. 3. The calculated data for Y_s using the same circular coaxial line with bevel angles 0°, 30°, 45°, and 60° with water ($\epsilon = 76 - i11.5$) as a calibration medium are obtained from (9) and are listed in Table I.

Experimental Results

The assembled laboratory test systems as used are shown in Fig. 4. The measurements are performed by using a six-port reflectometer (SPR), a low-cost laboratory computer and a number of standard microwave laboratory instruments (power meters, counters, sweepers, etc.) as presented in [9]. The equivalent model of the probe immersed into a tested medium is shown in Fig. 5. A short section of coaxial line L is used to model the effect of radiation of the electromagnetic fields in the tested medium from the probe [9]. The probes are calibrated by using two standard dielectric media, i.e., air and water ($\epsilon' = 76$, $\epsilon'' = -11.5$) and two different dimensions of the probes: $b_o = 0.0456$ cm, $b_1 = 0.1499$ cm, and $b_o = 0.0255$ cm, $b_1 = 0.0838$ cm, are tested. The calibration procedure and formulas are the same as in [9], and they will not be repeated here. The relationship between the normalized admittance at the open end of the probe, Y_s, the measured dielectric constant, ϵ, and the length of the coaxial line in the equivalent model (Fig. 5) is described by the

TABLE II
Comparison of Calculated and Measured Ratios $L(\varphi°)/L(0°)$ for $b_o = 0.0456$ cm, $b_1 = 0.1499$ cm by Using Air and Water as Standard Media

Frequency GHz	$L(45°)/L(0°)$		$L(60°)/L(0°)$	
	Calculated	Measured	Calculated	Measured
2.0	1.399	1.631	1.937	2.005
2.5	1.410	1.644	1.947	2.014
3.0	1.415	1.615	1.916	1.969
3.5	1.414	1.536	1.871	1.850
4.0	1.405	1.386	1.783	1.639

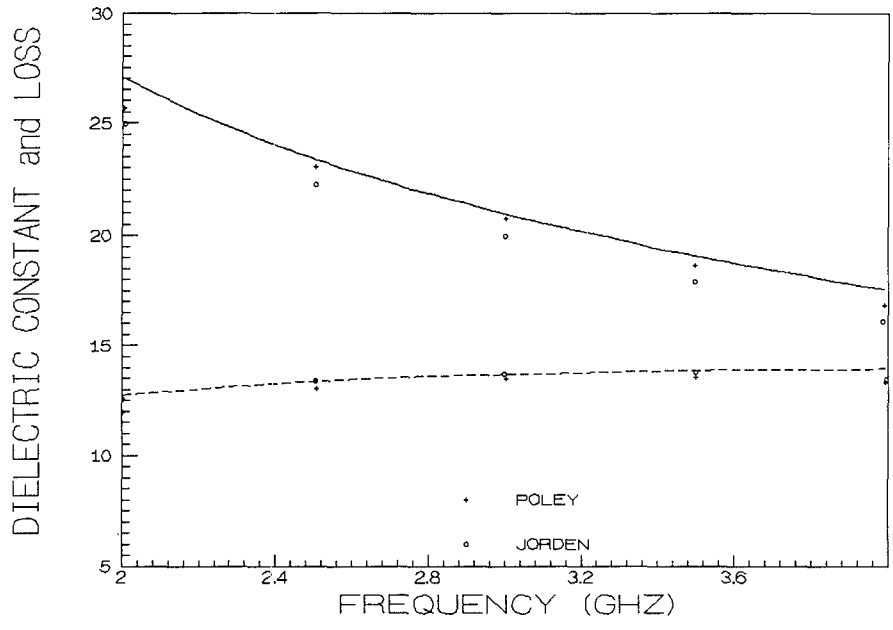

Fig. 6. Measured ϵ' and ϵ'' of methanol, $\varphi = 30°$ Legend: +Poley [11], o Jorden [12], —— our measurement (ϵ'), and ---- our measurement (ϵ'').

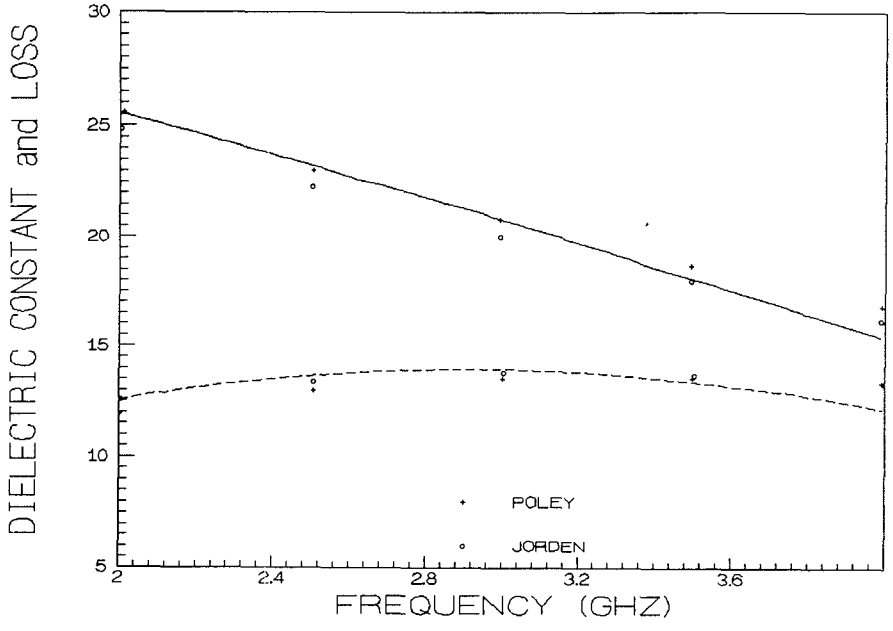

Fig. 7. Measured ϵ' and ϵ'' of methanol, $\varphi = 45°$ Legend: +Poley [11], o Jorden [12], —— our measurement (ϵ'), and ---- our measurement (ϵ'').

following formula:

$$Y_s = i\frac{\sqrt{\epsilon}}{\sqrt{\epsilon_t}}\tan\left(k_o\sqrt{\epsilon}L\right) \approx i\frac{\epsilon k_o L}{\sqrt{\epsilon_t}}. \tag{15}$$

The comparison of values $L(\varphi°)/L(0°)$ calculated and measured by using air and water as standard media for $b_o = 0.0456$ cm and $b_1 = 0.1499$ cm is shown in Table II.

The calculated data in Table II are obtained from the values Re(I) by using (9) and (15). It is noted that in general the degree of agreement increases with increasing bevel angles and as the elliptical model of the probe becomes more representative of the actual geometry of the probe tip.

This discrepancy is attributed to the following: the effect of higher order modes, the differences between the calculated and experimental models, the reflection of the transition from circular to elliptic coaxial line, the effect of the flange, the effect of radiation and measurement errors, etc.

Preliminary results were published in [10] and we now present finalized results. The experimental curves of dielectric constants of methanol over the frequency band 2–4 GHz using probes with bevel angles 30°, 45°, and 60°

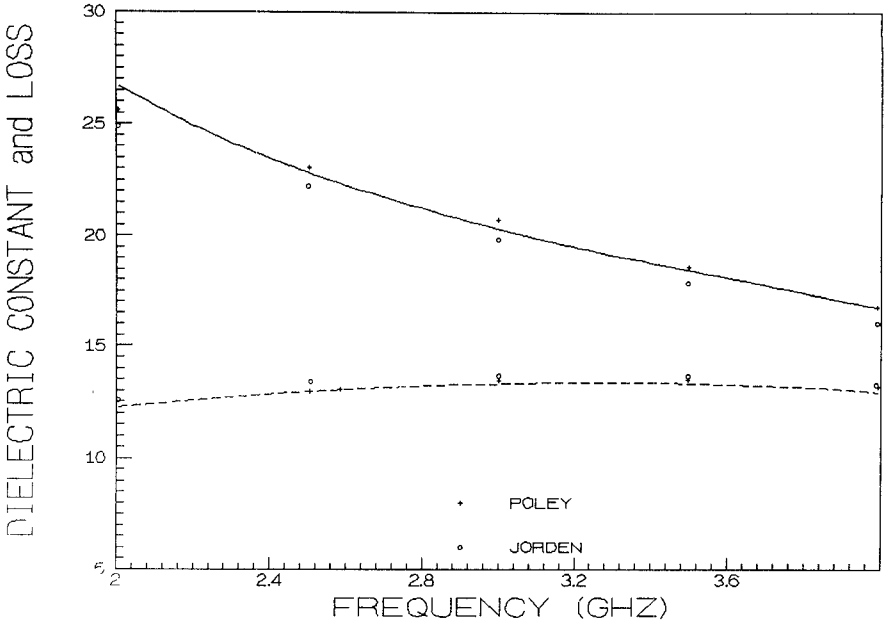

Fig. 8. Measured ϵ' and ϵ'' of methanol, $\varphi = 60°$ Legend: + Poley [11], o Jorden [12], —— our measurement (ϵ'), and ---- our measurement (ϵ'').

and their comparison with data published in the literature [11], [12] are shown in Figs. 6–8. In general, good agreement between the two sets of results is obtained.

The experimental curves of the same medium (methanol) measured by using standard coaxial probes (with bevel angle $\varphi = 0°$) are presented in [9] and they will not be repeated here. From the comparison of the above results, we conclude that both the standard and the beveled angle probes can give satisfactory experimental results which are in good agreement with each other. However the main advantages of the beveled probe are the following:

1) The measurement sensitivity increases with respect to the bevel angle for a given dimensioned circular coaxial line. This is especially valuable in cases of low frequency measurements and small dimensions of the probes where the sensitivity is low. Generally speaking, the measurement sensitivity is approximately proportional to the values of I, calculated from (9) or the length L in (15). When the probes are small, the sensitivity is actually proportional to I_1 in (10), where the higher order terms $I_3, I_4 \cdots$ are all very small and can be neglected. This is easy to understand since, for a certain probe and a certain amount of change of dielectric constant of the measured media, the larger I, L or I_1 will give larger changes of measured normalized admittance Ys. From Tables I, II, and Fig. 3, it is clear that all these three values (I, L and I_1) increase with the bevel angle φ. In general, improvement of 40% may be achieved in the case $\varphi = 45°$ in comparison with the standard probe ($\varphi = 0°$) and 90% in the case $\varphi = 60°$. It is also well-known that the measurement sensitivity increases with the dimension (cross-section) of the coaxial line.

2) A slanted cut aperture from a circular coaxial line (the beveled probe) is not only a practical model for the realization of probe tips with elliptical cross-section but it is also more valuable than a right angle cut aperture made on an elliptical coaxial line. The fabrication of the beveled probe is much simpler than the elliptical probe. More important is the fact that the beveled probe is much more useful than the probes used to date. In biological as well as biochemical applications, *in vivo* measurements of biological tissues on a living body are often essential. Nevertheless, the shape of a living body is generally quite complicated and the problem of fitting the probe into the measured sample often arises. By selecting the bevel angle φ, this fitting problem may be drastically facilitated and this feature is an additional advantage of this new type of probe, which is very important in biological measurements.

Conclusion

We have analysed an open-ended coaxial probe with an elliptic cross-section. Calculated and experimental results show that by using this kind of probe the measurement sensitivity may be improved, but at the same time, the radiation effect is also enhanced, especially at high frequencies. The beveled circular coaxial probe is a practical model for the realization of probe tips with elliptical cross-sections. It may not only drastically simplify the fabrication of this type of probe, but also makes it easier to insert the probe into the sample such as living tissues which is very important in biological as well as biochemical applications. Experiments show that the beveled angle probe has given satisfactory results, and it is a valuable asset in microwave permittivity measurements. The precise theoretical calculation of this probe is very complicated and the above theoretical analysis (radiation from open-ended elliptic coaxial line) is nevertheless useful.

The effects of higher order modes and the reflection of the transition from circular to elliptic coaxial line should be considered in the future. The present method of theoretical analysis is also useful in the study of radiation characteristics (impedance, gain, radiation patterns) of open-ended elliptic coaxial line antennas.

References

[1] Dr. G. Mariutti, Istituto Superiore di Sanita, Roma, Italia, Aug. 8, 1990, private communication.

[2] M. A. Stuchly *et al.*, "Measurement of radio frequency permittivity of biological tissues with an open-ended coaxial line: Parts I and II," *IEEE Trans. Microwave Theory Tech.*, vol. MTT-30, pp. 82–92, Jan. 1982.

[3] E. C. Burdette *et al.*, "In vivo probe measurement technique for determining properties at VHF through microwave frequencies," *IEEE Trans. Microwave Theory Tech.*, vol. MTT-28, pp. 414–427, Apr. 1980.

[4] D. Misra *et al.*, "Non invasive electrical characterization of materials at microwave frequencies using an open-ended coaxial line: Test of an improved calibration technique," *IEEE Trans. Microwave Theory Tech.*, vol. MTT-38, pp. 8–13, Jan. 1990.

[5] J. Galejs, *Antennas in Inhomogeneous Media*. New York: Pergamon, 1969, pp. 39–41.

[6] M. J. King and J. C. Wiltse, "Coaxial transmission lines of elliptical cross-section," *IRE Trans. on Antennas and Propagation*, vol. AP-9, pp. 116–118, Jan. 1961.

[7] J. A. Stratton, *Electromagnetic Theory*. New York: McGraw-Hill, 1941, pp. 52–54.

[8] D. K. Misra, "A quasi-static analysis of open-ended coaxial lines," *IEEE Trans. Microwave Theory Tech.*, vol. MTT-35, pp. 925–928, Oct. 1987.

[9] F. M. Ghannouchi and R. G. Bosisio, "Measurement of microwave permittivity using a six-port reflectometer with an open-ended coaxial line," *IEEE Trans. Instrum. Meas.*, vol. 38, no. 2, pp. 505–508, Apr. 1989.

[10] F. M. Ghannouchi, R. G. Bosisio, and R. Guay, "A comparative study on sensitivity analysis of various open-ended coaxial line geometries," in *Proc. 21st Symposium on Electrical Insulating Materials* 1988, pp. 103–107.

[11] J. P. Poley, "Microwave dispersion of some polar liquids," *Applied Scientific Research (B)*, vol. 4, pp. 337–387, 1955.

[12] B. P. Jordan, R. J. Sheppard, and S. Szwarnowski, "The dielectric properties of formamide, ethanediol and methanol," *J. Phys. D: Appl. Phys.*, vol. 11, pp. 695–701, 1978.

[13] J. R. Mosig, J. C. E. Besson, M. Gex-Fabry, and F. E. Gardiol, "Reflection on an open-ended coaxial line and application to non-destructive measurement of materials," *IEEE Trans. Instrum. Meas.*, vol. IM-30, pp. 46–51, 1981.

Yansheng Xu graduated from Tsing Hua University, Beijing, China in 1952.

From 1952 to 1957 he was engaged in research and development of microwave and radio communication equipment. From 1957 to 1961 he engaged in postgraduate studies and research work in the field of electrodynamics of gyromagnetic media and microwave ferrite devices at the Institute of Radio Physics and Electronics, Academy of Science, Moscow, USSR, and he received the degree of Candidate of Technical Science. In 1961 he joined the Beijing Institute of Radio Measurement. His main research interests include microwave measurement techniques, numerical methods of analysis and computer-aided design of microwave/millimeter wave integrated and monolithic circuits, electromagnetic fields, microwave ferrite devices, microwave ovens and microwave antennas.

He is Fellow of the Chinese Institute of Electronics (CIE) and he has published over 50 technical papers in his field of interest.

Fadhel M. Ghannouchi (S'84–M'88) received the degree in physics/chemistry in 1980 from the University of Tunis, Tunisia, Africa and the B.Eng. degree in engineering physics and the M.Eng. and Ph.D. degrees in electrical engineering in 1983, 1984 and 1987, respectively, from Ecole Polytechnique de Montréal, Montréal, PQ, Canada.

He worked as a Lecturer from 1984–1986 at Ecole Polytechnique de Montréal, where he taught electromagnetics microwave theory and techniques. Since 1987, he has been a Senior Research Associate at the Microwave Research Laboratory of Ecole Polytechnique. Since 1990 he was appointed Assistant Professor with the same laboratory. His research interests are microwave/millimeter-wave metrology and CAD/CAM of microwave/millimeter-wave devices and circuits for satellite and mobile communications equipment with special emphasis on six- port measurement techniques and nonlinear circuits.

Dr. Ghannouchi is a registered professional engineer in province of Quebec, Canada. Dr. Ghannouchi is on the editorial board of IEEE TRANSACTIONS ON MICROWAVE THEORY AND TECHNIQUES.

Renato G. Bosisio (M'79–SM'89) was born in Italy in 1930. He received the B.Sc. degree from McGill University, Montreal, PQ, Canada, in 1951, and the M.S.E.E. degree from the University of Florida, Gainesville, in 1963.

He has been engaged in microwave research and development work with various firms: Marconi and Varian in Canada, Sperry in the U.S., and English Electric in England. He is presently the Head of the Section d'Electromagnétisme et d'Hyperfréquences at Ecole Polytechnique de Montréal, Montréal, Canada, where he teaches microwave theory and techniques. He is actively engaged in six-port technology, dielectric measurements, and the computer-aided testing and design of both active and passive microwave devices.